Metallic state and the metal-insulator transition of $NdNiO_3$

X. Granados, J. Fontcuberta, and X. Obradors
Institut de Cîencia de Materials de Barcelona, Consell Superior de Investigacions Científiques, Campus Universitat Autònoma de Barcelona, 08193 Bellaterra, Spain

Ll. Mañosa
Departament d'Estructura i Constituents de la Matèria, Facultat de Física de la Universitat de Barcelona, Diagonal 647, 08028 Barcelona, Spain

J. B. Torrance
IBM Research Division, Almaden Research Center, 650 Harry Road, San Jose, California 95120-6099
(Received 19 February 1993)

We report detailed measurements of the electrical resistivity, Seebeck coefficient, and differential scanning calorimetry across the metal-insulator (MI) transition ($T_{MI} \approx 205$ K) of $NdNiO_3$. As in the isostructural oxide $PrNiO_3$, the transition is extremely hysteretic, consistent with the first-order character of the transition. Analysis of the data shows that metallic and nonmetallic phases coexist in a broad temperature interval (≈ 70 K). The electrical resistivity and Seebeck coefficients of the metallic state display a clear linear temperature dependence. These properties can be rationalized in terms of a Fermi gas picture of rather heavy electrons (effective mass of about $6m_0$). Some physical parameters of the gas are predicted. The entropy change across the MI transition has been measured and it has been used to predict a strong pressure dependence of the MI transition temperature: $dT_{MI}/dP \approx -4.8$ K/kbar.

I. INTRODUCTION

The electronic structure and the transport properties of the transition-metal oxides have become a major topic of research. Interest in them was triggered by the discovery of superconductivity in cuprate oxides and serious revisions of the currently accepted models to describe the insulating nature of the nondoped materials have been proposed. One of the most fundamental issues to be solved is probably the origin of the band gap and the mechanisms leading to a metallic conductivity when doping.

Zaanen, Sawatzky, and Allen[1] proposed a general scheme to describe the nature of the insulating state in transition-metal oxides. The band gap can arise either from the $3d$-$3d$ Coulomb energy U (i.e., Hubbard-Mott insulators) or from the charge-transfer energy Δ between O($2p$) and metal ($3d$) bands (i.e., charge-transfer insulators). Accordingly, two types of metal-insulator (MI) transitions can be expected in pure materials: when the Hubbard-Mott band gap or when the charge-transfer gap closes. Layered cuprates are believed to be charge-transfer insulators. However, in these systems metallic conductivity is reached through a heavy doping which should strongly disrupt the electronic band structure, thus rendering the material intrinsically nonideal to study the nature of the metal-insulator transition.

Recently, it has been shown[2] that nickel oxides of the $RNiO_3$ (R =Nd,Sm,Eu,Pr) family, which are metallic at high temperature, display a metal insulator transition at temperatures T_{MI}. It has been claimed that in the insulating regime the band gap is also of charge-transfer type, the highest-energy occupied orbitals being of O($2p$) parentage are separated from the empty orbitals of Ni($3d$) parentage by the charge-transfer energy Δ.[3] The MI transition would result from the band gap closing and eventually from the O($2p$) and Ni($3d$) bands overlapping that occur because of the lattice contraction at low temperatures.[4]

It is well established that the MI transition is weakly first order[4,5] and the transition temperature T_{MI} rises systematically as the size of the rare earth decreases.[2,4] For R =La the system remains metallic down to 1.5 K, whereas for R =Pr, Nd, Sm, and Eu electron localization occurs at 135, 200, 400, and 460 K, respectively. Recent neutron-diffraction experiments[5] on Pr and Nd have shown that the MI transition is accompanied by small structural changes that take place at T_{MI}. The first-order character of the electronic transition is shown by the sudden, although small ($\leq 0.25\%$), volume expansion of the lattice when electron localization occurs.[5] It has also been shown that across the MI transition, expansion of Ni-O bond length due to loss of metallic bonding leads to a slight tilt of the Ni-O-Ni angles ($\Delta\theta_{MI} \approx -0.5°$).

Neutron-diffraction data have also revealed that in $PrNiO_3$ and $NdNiO_3$ below T_{MI} some extra, weak reflections of magnetic origin appear.[6] However, in the highly distorted compounds such as $SmNiO_3$ and $EuNiO_3$ there is a clear separation between the metal-insulator transition and the Néel temperature.[4] Therefore the possibility of a band gap of antiferromagnetic (AF) origin in this family of oxides seems to be unlikely, although at the present stage it cannot be completely disregarded. On the other hand, in $PrNiO_3$ and $NdNiO_3$ the saturated magnetic moments[2,6] are consistent with Ni^{3+} low-spin state for nickel rather than high-spin Ni^{2+} and holes on the oxygen sites.

We have recently investigated[7] the pressure dependence of T_{MI} by using electrical resistance measurements. We have found that, in spite of the differences in T_{MI} (100–200 K), for all investigated materials (R =Nd,Pr,$Nd_{1-x}La_x$) the transition temperature decreases under pressure with a common rate $dT_{MI}/dP \approx -4.2$ K/kbar.

In order to understand the nature of the band gap and to build up the appropriate ground state for the electronic structure, it is important to know the character of the majority charge carriers in both the metallic and the insulating phases and the magnitude of the gap. Associated with the first-order MI transition, a coexistence of the high-temperature metallic phase and the low-temperature semiconductor phase over a certain temperature range close to the MI transition could be expected[8] thus leading to an hysteretic behavior of the transport properties. Analysis of the transport coefficients in the hysteretic region can provide an estimate of the relative thermodynamic stability of both phases. In $PrNiO_3$ we have found that hysteresis as measured by the transport coefficients extends over some 40 K. The coexistence of the metallic and insulating phases may be relevant to the interpretation of several experimental results and it is important to evaluate to which extent both phases coexist.

In this paper we report detailed measurements of the electrical resistivity and Seebeck coefficient across the MI transition in ceramic $NdNiO_3$ pellets. We will show that charge carriers are electronlike and their character does not change across the transition, which occurs at $T_{MI} \approx 205$ K. Transport data reveal hysteresis effects. We will show that there is a broad temperature range, larger than 70 K, well below the onset of the MI transition, where metallic regions of the sample coexist with semiconducting ones. Moreover, we will show that the rate of the MI phase transformation can be extracted from Seebeck, conductivity, and differential scanning calorimetry (DSC) data. The transport properties in the metallic state will be discussed and we will show that they can be rationalized in terms of a Fermi-gas picture of rather heavy electrons. Some physical parameters of the gas (specific heat coefficient, effective mass, etc.) have been evaluated. The entropy change across the MI transition has been measured and it has been used to predict a strong dependence of T_{MI} on pressure. Furthermore, this estimate of dT_{MI}/dP is in excellent quantitative agreement with the available experimental data.

II. EXPERIMENT

$NdNiO_3$ powder was prepared by synthesis under high oxygen pressure. Details of the synthesis can be found elsewhere.[2] X-ray and neutron-diffraction experiments show that the material is well crystallized, single-phase, and has a perovskite structure.[2] The ideal cubic symmetry of the perovskite is slightly distorted leading to a lower-symmetry structure. Extensive structure analysis has been reported elsewhere.[2,5,6]

Resistance measurements were performed by the four-probe technique, inverting current polarity in order to correct the offset of the amplifiers and thermoelectric contributions. Measuring currents in the 500 nA–5 mA range were used with identical results. Measurements were done in a He closed-cycle cryostat from room temperature down to 10 K. The temperature stability during the resistance measurements is better than ±0.05 K. All the data reported here have been taken in a measuring protocol which involves temperature sweeps with a constant cooling or heating rate of 0.3 K/min.

Seebeck measurements were performed using an experimental system developed in our laboratory in the liquid nitrogen to room-temperature range. The difference in temperature along the sample during each Seebeck measurement rises up to 2 K.

Differential scanning calorimetry measurements were performed using a high-sensitivity differential microcalorimeter (about 400 mV W^{-1} at room temperature) described elsewhere.[9] The temperature range of operation is limited from around 100 to 370 K. The heat exchanged and the entropy change associated with a phase transition are obtained by numerical integration of the recorded thermal curves, after correction for the calorimetric base line.

III. RESULTS

A. Electrical resistance

The general behavior of the electrical resistance versus temperature, $R(T)$, is shown in Fig. 1. The solid circle experimental points correspond to data recorded in a heating process. This figure clearly shows that above $T_{MI} \approx 205$ K, $R(T)$ has a constant positive slope thus indicating a metallic behavior. At high temperature (300 K) the resistivity is $\rho \approx 1.2$ mΩ cm and the normalized resistance slope $1/R\,(dR/dT)$ is 3.5×10^{-3} K^{-1}, which is a rather high value and comparable to that typically observed in good metals (for instance, Cu: 6×10^{-3} K^{-1}). At low temperature a semiconductinglike temperature dependence is observed with a sudden enhancement of the resistivity of about three orders of magnitude in a temperature interval of 10 K. The onset of semiconduct-

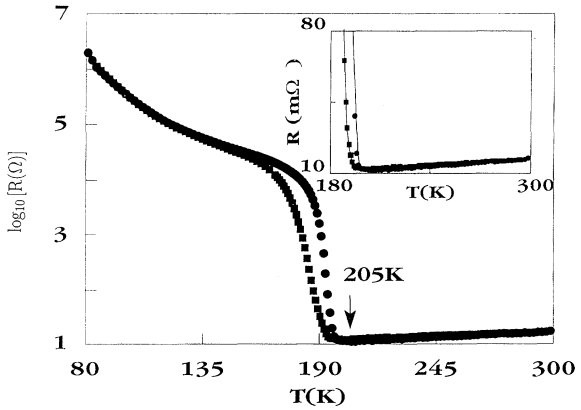

FIG. 1. Electrical resistance vs temperature for $NdNiO_3$, measured in heating (solid circles) and cooling (solid squares) cycles. The arrow indicates the onset temperature T_{MI} of the metal-insulator transition. Inset: detail of the transition. Notice the different y-axis scales in both plots.

ing behavior is extremely abrupt (see inset of Fig. 1) and the temperature $T_{MI} \approx 205$ K, where the transition from metal to insulator takes place, is well defined. If the data are plotted in a $\log_{10}(R)$ vs $1/T$ scale, as in Fig. 2, the low-temperature part ($T < 140$ K) displays a smooth curvature, which indicates that a simple activated behavior is only a crude description of the low-temperature behavior. From the slope of this curve in the 150–120-K temperature range, we estimate that the activation energy is about 25–28 meV. Inspection of Fig. 2 reveals that $\log_{10}(R)$ vs $1/T$ has an upwards curvature and thus the slope, i.e., the activation energy, increases when lowering the temperature. In terms of a semiconductorlike band-gap model it means that the band gap increases rapidly at lower temperature.

Figure 1 also shows the measured resistance in the cooling process (recorded at the same temperature variation rate of 0.3 K/min). The hysteretic behavior of $R(T)$ is clearly observed and it provides a beautiful manifestation of the first-order character of the MI transition. The cooling curve always displays a lower resistivity. This fact signals the persistence of nuclei of the high-temperature metallic phase below the onset of the MI transition. It can be appreciated in Fig. 2 that the temperature at which the metallic behavior is established or disappears is well defined but depends slightly on the sense of the thermal cycle. Within the experimental resolution, this difference can be estimated as about 1 K. We have not found any measurable dependence of T_{MI} on the rate of cooling or heating of the sample. At temperatures below 130 K no trace of hysteresis is observed.

In the lower-temperature part of the metallic region, very small differences between the resistances in the cooling and the warming processes can be observed. These differences disappear at higher temperature and are probably due to very subtle changes in the ceramic structure caused by the phase transition and its concomitant cell-volume changes.

B. Seebeck coefficient

Figure 3 shows the Seebeck coefficient $S(T)$ measured from 300 K down to 80 K, where the sample is kept for 4 h and heated again to 300 K. At high temperatures, $S(T)$ has a linear temperature dependence; it is small in magnitude and negative (≈ -22 μV/K at 205 K). This behavior is typical of a metallic state with electronlike particles as charge carriers. The observation of a linear $S(T)$ behavior further indicates that the dominant scattering mechanism and the charge-carrier density are constant over the explored temperature range. Within the relaxation-time approximation, the Seebeck coefficient is given by[10]

$$S(T) = -\frac{\pi^2 k^2}{3e} T \left[\frac{g(\varepsilon)}{n} + \frac{\partial}{\partial \varepsilon} \ln[\tau(\varepsilon)] \right]_{\varepsilon = E_F}, \quad (1)$$

where $g(\varepsilon)$ is the density of states, n is the charge-carrier density, and E_F is the Fermi energy. $\tau(\varepsilon)$ is the energy-dependent relaxation time, which, in general, can be written as $\tau(\varepsilon) \sim \varepsilon^{\alpha}$, where the exponent α is related to the scattering mechanism. Assuming a parabolic band and for the particular case of $\alpha \approx -1$, the simplest Drude expression

$$S(T) = -\frac{\pi^2 k^2}{6e} \frac{T}{E_F} \quad (2)$$

is recovered whereas for an energy-independent scattering time

$$S(T) = -\frac{\pi^2 k^2}{2e} \frac{T}{E_F} \quad (3)$$

is obtained. By using the Drude expression [Eq. (2)], the observed slope of $S(T)$ in the metallic regime [$dS(T)/dT \approx -0.029$ μV/K^2] corresponds to a Fermi energy $E_F \approx 0.41$ eV. This rather small value of E_F is similar to the previously reported data ($E_F \approx 0.40$ eV) for $PrNiO_3$ (Ref. 8) and ($E_F \approx 0.21$ eV) for $LaNiO_3$ (Ref. 11) and contrasts with the higher values typically observed in normal metals, for instance, E_F (Cu) ≈ 7 eV. If the relaxation time is energy independent the Seebeck coefficient [Eq. (3)] is three times larger and the corresponding Fermi energy is about $E_F \approx 1.2$ eV.

In the cooling part of the cycle, the metallic regime is observed down to $T \approx 195$ K. At lower temperature $S(T)$ decreases abruptly, becoming very large in magni-

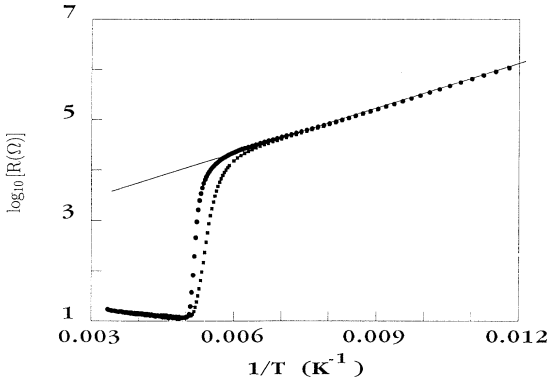

FIG. 2. Electrical resistance vs $1/T$ of $NdNiO_3$. Below 150 K, $\log_{10}(R)$ has an upward curvature. Circles and squares correspond to data recorded in the heating and cooling cycles, respectively.

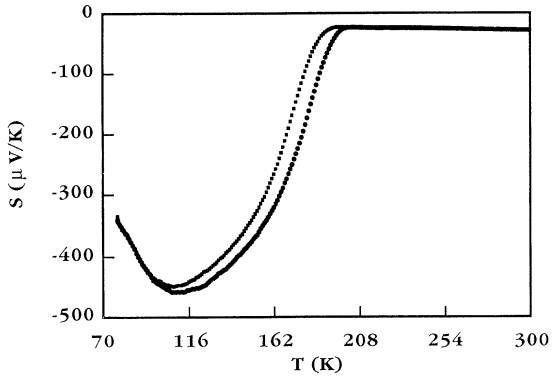

FIG. 3. Seebeck coefficient S vs temperature. Circles and squares correspond to data recorded in the heating and cooling processes.

tude ($S \approx -470$ μV/K at 110 K). Larger Seebeck coefficients are typical of a semiconductorlike state because of the smaller charge-carrier density. Therefore our Seebeck data clearly reflect the MI transition. It is remarkable that in the insulating side of the transition the majority charge carriers are also electronlike. At temperatures lower than 110 K, the absolute value of the Seebeck coefficient diminishes, signaling that the dominant mechanism is not semiconductorlike or that a regime of charge compensation is present.[12] When warming up (see Fig. 3), S decreases again until a minimum is reached at $T \approx 110$ K and then approaches the metallic regime. However, the fully metallic state is only reached at $T \approx 200$ K, which is only a few degrees lower than the temperature where the MI transition was observed in the $R(T)$ curves. As expected, the persistence of some metallic nuclei close to, but below, T leads to smaller (in magnitude) $S(T)$ values when cooling than when heating.

C. Differential scanning calorimetry

Figure 4 shows the thermal energy released and absorbed during the cooling and heating runs, respectively. As expected for a first-order phase transition, the cooling process is exothermic whereas the heating process is endothermic. The values obtained for the enthalpy and entropy changes are $\Delta H \approx -237$ J mol^{-1} and $\Delta S \approx -1.3$ J K^{-1} mol^{-1} for the cooling run and $\Delta H \approx 353$ J mol^{-1} and $\Delta S \approx 1.8$ J K^{-1} mol^{-1} for the reverse transition. The apparent differences observed between the values obtained in the cooling process and the ones obtained in the heating process are mostly associated with the fact that the enthalpy change ΔH is temperature dependent. This difference stems from the difference in the specific heat between the two phases, that is, $\partial \Delta H / \partial T = \Delta C_p$. Therefore the term $\int \Delta C_p dT$ must be included in the energy balance. From Fig. 4 we have estimated ΔC_p to be 13 J K^{-1} mol^{-1}, and $\int \Delta C_p dT$ is about 70 J K^{-1} mol^{-1}. Consequently, the measured enthalpy difference between the cooling and heating cycles is only about 55 J mol^{-1}. The smaller residual difference ($\approx 15\%$) is within the accuracy of the experimental setup.

The transformed fraction of the sample is proportional to the normalized entropy change at this temperature:

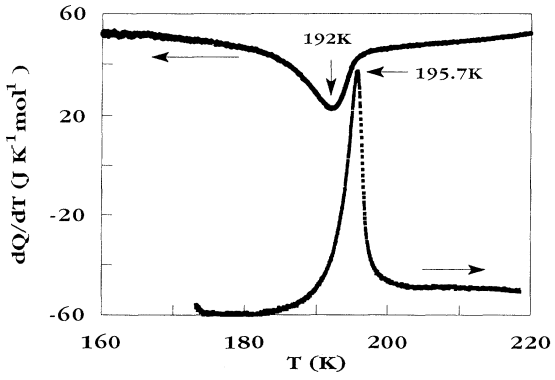

FIG. 4. Heat released and absorbed in the cooling (solid circles) and heating (solid squares) processes, respectively.

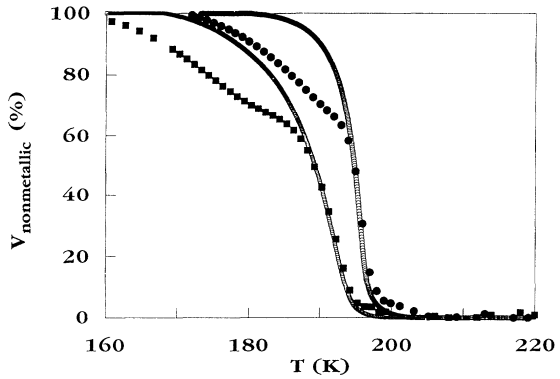

FIG. 5. Volume fraction of the nonmetallic phase deduced from resistivity (solid symbols) and DSC (open symbols) data. Squares and circles correspond to cooling and heating processes, respectively.

$m = \Delta S(T)/\Delta S(\text{total})$. The transformed fraction of nonmetallic phase m is plotted in Fig. 5. This figure clearly reveals the thermal hysteresis inherent to the first-order character of the transition. The onset of the forward (metallic to insulator) transformation in the cooling run is situated at 200 K and the onset of the reverse (insulator to metallic) transition occurs at 203 K. These values are in perfect accordance with the ones obtained through resistivity measurements.

It must be pointed out that the last stages of the forward transition are very smooth, i.e., small regions of the sample transform in a broad temperature range, resulting in small energy release which extends over a broad temperature interval. Some of this energy will be below the limit of detectability of the calorimeter. This fact may also account for the smaller enthalpy values obtained in the cooling run.

IV. DISCUSSION

The experimental data reported above provide relevant information on different aspects of the MI transition, which we will discuss in turn. First, the hysteretic behavior of the resistivity and Seebeck data across the MI transition will be considered. We will show that transport data can be used to deduce the rate of phase transformation, which turns out to be in good agreement with the calorimetric data, thus indicating that the transport coefficients [$R(T)$ and $S(T)$] indeed measure an intrinsic property of the phase transformation and are not seriously affected by the ceramic nature of the investigated samples. Second, we will address the question of the magnitude and sign of the Seebeck coefficient and we will show that these data provide a new insight into the electronic properties of the metallic phase. Finally, the magnitude of the enthalpy and entropy changes across the transition will be discussed and we will show that they provide a quantitative description of the dependence of the metal-insulator transition temperature with pressure.

The hysteretic behavior of the transport coefficients across the MI transition is a clear signature of the first-order character of this transition. The relative rate of phase transformation and thus the concentration of both

species (I and M) at each temperature determine the overall shape of the $R(T)$ and $S(T)$ curves and their hysteresis. As is observed in $PrNiO_3$,[8] the evolution of the transport properties across the transition can be interpreted by assuming that the material is a blend of two components with different transport characteristics, a metallic phase and an insulating phase. We can deduce the proportion of both phases from resistivity data.

Basically, the overall conductivity (σ^*) of such a heterogeneous system depends on the conductivities of the components (σ_1,σ_2), on their geometries, and on their distribution. Several expressions have been proposed in order to calculate σ^* in terms of σ_i ($i=1,2$) and the relative volume V_i ($i=1,2$) of each phase.[13] The usual approximations assume that the particles are immersed in a homogeneous medium of conductivity σ' which is interpreted as the overall conductivity σ^* and constructed self-consistently. In the particular case of spherical particles and in the framework of the symmetrical effective medium theory of Bruggeman,[13] $\sigma^*$is given by

$$V_1[(\sigma_1-\sigma^*)/(\sigma_1+2\sigma^*)] + (1-V_1)[(\sigma_2-\sigma^*)/(\sigma_2+2\sigma^*)]=0 . \quad (4)$$

In order to use Eq. (4) to extract the volumes of each phase, the values of $\sigma_1(T)$ and $\sigma_2(T)$ are needed. For that purpose we have fitted the high- and low-temperature data, well above and below T_{MI}, to some analytical expressions which are used to extrapolate the data in the region of interest, i.e., close to T_{MI}. Extensive details of the data analysis can be found in Ref. 8. Figure 5 shows the volume of nonmetallic phase as deduced from Eq. (4), assuming that the behavior of both phases in the transition interval of temperature may be represented by the extrapolation of their behavior in the regions where they exist alone. Comparison of data in Fig. 5 shows an excellent agreement between the transport and calorimetric determinations of V_i when the relative volume of the nonmetallic phase is less than $\approx 65\%$, that is, a metallic relative volume larger than 35%. At higher concentration the symmetrical effective medium model is expected to break down.[13] Applicability of Eq. (4) should be limited by the loss of percolation of the metallic nuclei, which is predicted to occur at about $V_M \approx 35.\%$[13] Below the percolation threshold of the metallic phase, the estimates from resistance measurements lead to a slightly higher proportion of metallic phase than from DSC data.

We come now to electron-transport coefficients. Above T_{MI} resistivity and Seebeck coefficients have a linear temperature dependence. The normalized resistivity slope is comparable to that commonly found in good metals. Both behaviors are expected in a normal metal and can be easily understood in terms of a Fermi-gas picture, which is thus an appropriate starting point for our analysis.

In the parabolic band approximation, the calculated Fermi energy $E_F=0.41$ eV can be combined with the electron density n to obtain the density of states $g(E_F)$ at the Fermi level. Assuming an electron per Ni atom (Ni^{3+}, $t_{2g}^6 e_g^1$) (Ref. 6) and the cell volume $V_c \approx 220$ Å^3,[5] then $n \approx 1.8\times 10^{22}$ cm^{-3}, which, together with $E_F=0.41$ eV, leads to $g(E_F)\approx 6.5\times 10^{11}$ eV^{-1}cm^{-3}. This density of states can be compared to the bare $g^0(E_F)$ corresponding to free electrons and which can be calculated from n. It turns out that $g^0(E_F)\approx 1.08\times 10^{22}$ eV^{-1}cm^{-3}. The ratio $g(E_F)/g^0(E_F)$ is a measure of m^*/m_0, the ratio of the effective electron mass (m^*) to the free-electron mass (m_0). Therefore $m^*\approx 6m_0$. At the same level of approximation, the coefficient of the linear temperature term of the specific heat γ is predicted to be about 8.2 mJ/mol K^2. It can be significant that for $LaNiO_3$, which is also a metallic perovskite, electron spectroscopy studies[11] have suggested an effective mass for electrons in the region of $6m_0$, which is in good agreement with the present estimates.

To further check these predictions other experimental data are required, for instance, specific-heat measurements, which at present are lacking. However, comparison can be made with recently reported[14] calorimetric measurements on $LaNiO_3$, where $\gamma=13.8$ mJ/mol K^2 has been obtained. This result is in a reasonable agreement with our rather crude estimate. The fact that our estimate of γ for $NdNiO_3$ is smaller than that observed (for $LaNiO_3$) could be understood in terms of a semimetallic conduction of these oxides. In that case both electron and holes in the 3d-Ni and 2p-O bands, respectively, contribute to γ, although S is dominated by the carriers having higher mobility (the electrons).

The above estimates of the metallic parameters (m^*,γ) are based upon the assumption that the electron density is one electron per unit cell and the scattering rate is $\tau(\varepsilon)\sim\varepsilon^{-1}$. We can check these predictions as follows. We have measured[15] the Seebeck coefficient of a $LaNiO_3$ sample and its temperature dependence. It turns out that $dS(T)/dT\approx -5\times 10^{-8}$ V/K^2.

The ratio

$$\frac{\frac{dS(T)}{dT}}{\gamma}$$

can be evaluated by using Eq. (1) and the Sommerfeld expression[10] for γ; it turns out that it provides an independent estimate of n. In the particular case of $\alpha=-1$,

$$\frac{\frac{dS(T)}{dT}}{\gamma}=-\frac{1}{3ne} . \quad (5)$$

By using our measured value of the slope of $S(T)$ and $\gamma=13.8$ mJ/mol K^2 we obtain $n\approx 1.7\times 10^{22}$ cm^{-3}. It is remarkable that this value is close to the density which one can estimate by assuming one electron per Ni atom in $LaNiO_3$.

It should be noticed that if an energy-independent scattering rate were used, then the corresponding $[dS(T)/dT]/\gamma$ rate gives an electron density three times larger, which will correspond to an explicit higher electron density (≈ 3 electrons per unit cell). Therefore it is reasonable to use the Drude expression [Eq. (2)] and the consistency of the estimates of m^* and g given above is

reinforced. These similarities provide additional support to the picture of the metallic properties in terms of a Fermi gas.

The discussion presented above reveals that, in the metallic phase, $NdNiO_3$ behaves essentially as a normal metal with electrons as charge carriers but having a substantial effective mass. However, our precise estimate of m^* is based upon the assumption that there is one electron per Ni atom participating to the conduction. If the metallic state in $NdNiO_3$ is reached by closing a charge-transfer gap, there should be much less than one conduction electron per Ni atom (since under such an assumption $NdNiO_3$ would be a semimetal). Thus the charge-transfer-gap scenario would have less carriers and hence a smaller $g(E_F)$. Consequently, m^* will be correspondingly reduced. At present, because a direct determination of the charge-carrier density is lacking, the estimate of m^* remains rather speculative and thus we cannot be conclusive in this regard. To what extent the coincidence of pure crude evaluation of m^* and the value inferred from electron-energy-loss spectroscopy[11] is fortuitous is still unknown.

Within the scope of the Brinkman-Rice model[16] for correlated electrons, the enhancement of the effective electron mass arises because the correlation energy U approaches a limiting value U_0 at which a correlation gap opens at the Fermi level. Explicitly,[16]

$$m^*/m_0 = 1/[1-(U/U_0)^2] . \quad (6)$$

Equation (6) is based on perturbation theory and it cannot be used for large m^*/m_0 ratios to make accurate quantitative estimates of U/U_0.[17] However, $m^* 6 m_0$ would indicate that the system is close to the metal-insulator transition. If the band gap in the insulating state is of charge-transfer type as suggested by Torrance *et al.*[4] and the metallic conductivity is reached via overlapping of the $2p$ and $3d$-like bands, then the enhanced effective mass would reflect only the narrow character of the $3d$-like bands.

However, our conclusion raises new questions, especially on the nature of the band gap that appears to be opened at T_{MI}. In terms of the model for metallic conduction at $T > T_{MI}$ suggested by Torrance *et al.*,[4] the overlapping of the oxygenlike p bands and the metallike d bands increases with temperature. Therefore one could expect that the density of charge carriers and/or their mobility should increase with temperature. At present a direct measure of the carriers's density is not available, but the observed linear temperature dependence of the resistivity and Seebeck coefficient as well as the reasonable estimate of γ suggest that the charge-carrier density does not change appreciably with temperature. The most obvious way to account for the available data in the metallic state and to avoid these difficulties would be, of course, electronic conduction in a single band. However, in such a case the nature of the band structure in the metallic state and thus the band gap remain open questions.

We turn now to the measured thermodynamical properties. The entropy and cell volume changes in the metal-insulator transition can be combined through the Clausius-Clapeyron equation to obtain the slope of the $T_{MI}(P)$ line separating the I and M phases in the P-T plane. By using the $\Delta S \approx -1.3\ \mathrm{J\,K^{-1}\,mol^{-1}}$, reported here, and $\Delta V \approx 0.2\%$ of Ref. 5, we obtain $dT_{MI}/dP \approx -5.4$ K/kbar. Recently we have performed a systematic study of the pressure dependence of the metal insulator transition in a series of nickel perovskites $RNiO_3$ (R =Pr,Nd,$La_{1-x}Nd_x$) and we have found that for all of them $dT_{MI}/dP \approx -4.2$ K/kbar.[7] This value is in an excellent agreement with our estimates, which are based on very general thermodynamical considerations. Furthermore, because the volume contraction across the MI transition[5] and dT_{MI}/dP are almost insensitive to the rare earth, the entropic change across T_{MI} should also be similar. Indeed, recent experimental determinations[15] of ΔS at T_{MI} in $SmNiO_3$ lead to $\Delta S = -1.3\ \mathrm{J\,K^{-1}\,mol^{-1}}$, which is very similar to the result obtained for $NdNiO_3$.

In $NdNiO_3$, magnetic, electronic, and phonon-related contributions to the entropy changes set in at T_{MI} because of the AF ordering that accompanies electron localization and lattice distortion. It is difficult at present to discriminate between these factors. The precise microscopic description of this state is far from being complete. So far, it is only known that a band gap should be opened in order to account for the existence of an insulating phase and there are conclusive indications[6] that a magnetic ordering of the Ni^{3+} spins ($S=\frac{1}{2}$) takes place at T_{MI}. The magnetic contribution (ΔS_M) to the overall entropy variation can be estimated by using $\Delta S_M \approx \beta R Ln(2S+1)$ where S is the spin of the Ni^{3+} ions and β is the fraction of them that contribute to the enhancement of ΔS_M. Assuming a fully saturated magnetic moment and taking $\beta=1$ (all Ni spins order at lower temperature), the maximum magnetic contribution to the entropy change is $\Delta S_M \approx -5.7$ J/mol K, which is somewhat larger than our experimental value. This result is rather surprising as one would expect the measured value to be larger than the magnetic contribution alone if it were relevant at all. In fact, the observation that ΔS in $SmNiO_3$, where the AF ordering temperature is well below T_{MI}, is very similar to that observed in $NdNiO_3$ rules out an important magnetic contribution to ΔS. At present we do not have conclusive arguments to account for the nonobservance of an appreciable magnetic contribution to the measured ΔS in $NdNiO_3$; however, some explanations can be suggested. First, if magnetic correlations exist above T_{MI}, where the antiferromagnetic long-range order sets in, then a reduced entropy change across T_{MI} should occur. Second, if the magnetic moment in the temperature range where the integration of dQ/T (≈ 150 K) has been performed has not reached its fully saturated value then a smaller entropy change should have been obtained.

V. CONCLUSIONS

In summary, we have shown that the hysteretic behavior observed in the transport and calorimetric data, which extends over a wide temperature range (≈ 70 K), below the metal-insulator transition ($T_{MI} \approx 205$ K), is related to the coexistence of both phases. The analysis of

the data has allowed us to extract the rate of phase transformation. It is relevant that this rate is severely reduced at low temperature, thus suggesting important effects of pressure on T_{MI}. The analysis of the calorimetric data has also provided a measure of the entropy change across the MI transition. It is remarkable that we have been able to predict a pressure dependence of T_{MI}, which is in excellent agreement with the recently reported data.

The nature of the electrical transport in the metallic state has been discussed on the basis of the Seebeck and resistivity data. We have shown that these nickel perovskites can be well described in terms of a Fermi gas of electrons of a rather high effective mass ($\approx 6m_0$). The significance of these results in terms of the already proposed models has been pointed out. New experiments aimed to provide the deeper insight into the metallic and insulating state of these fascinating materials are currently being carried out.

ACKNOWLEDGMENTS

We would like to acknowledge stimulating discussions with J. L. García-Muñoz. Financial support from the CEE (SCI-0389M(A) and 0036-F) and the Spanish CICYT-MIDAS program (Mat: 91-0742) is acknowledged.

[1]J. Zaanen, G. A. Sawatzky, and J. W. Allen, Phys. Rev. Lett. **55**, 418 (1985); J. Zaanen and G. A. Sawatzky, J. Solid-State Chem. **88**, 8 (1990).

[2]P. Lacorre, J. B. Torrance, J. Pannetier, A. I. Nazzal, P. W. Wang, and T. C. Huang, J. Solid-State Chem. **91**, 225 (1991).

[3]J. B. Torrance, P. Lacorre, C. Asavaroengchai, and R. M. S. Metzger, J. Solid-State Chem. **90**, 225 (1991); Physica C **182**, 351 (1991).

[4]J. B. Torrance, P. Lacorre, A. I. Nazzal, E. J. Ansaldo, and C. H. Niedermayer, Phys. Rev. B **45**, 8209 (1992).

[5]J. L. García-Muñoz, J. Rodríguez-Carvajal, P. Lacorre, and J. B. Torrance, Phys. Rev. B **46**, 4414 (1992).

[6]J. L. García-Muñoz, J. Rodríguez-Carvajal, and P. Lacorre, Europhys. Lett. **20**, 241 (1992); (unpublished).

[7]X. Obradors, L. Paulius, J. Fontcuberta, J. B. Torrance, and M. B. Maple (unpublished).

[8]X. Granados, J. Fontcuberta, X. Obradors, and J. B. Torrance, Phys. Rev. B **46**, 15 683 (1992).

[9]G. Guénin *et al.*, Proc. ICOMAT-86 (The Japan Institute of Metals), 794 (1987).

[10]N. W. Ashcroft and N. D. Mermin, in *Solid State Physics,* edited by D. G. Crane (Saunders, Philadelphia, 1976).

[11]J. P. Kemp and P. A. Cox, Solid-State Commun. **75**, 731 (1990).

[12]A. J. Bosman and C. Crevecoeur, Phys. Rev. **144**, 763 (1965).

[13]P. L. Rossiter, in *The Electrical Resistivity of Metals and Alloys,* edited by R. W. Cahn, E. A. Davis, and I. M. Ward, Cambridge Solid State Science Series (Cambridge University Press, Cambridge, England, 1991); R. Landauer, in *Electrical Transport and Optical Properties of Inhomogeneous Media,* edited by J. L. Garland and D. B. Tanner, AIP Conf. Proc. No. 40 (AIP, New York, 1978).

[14]K. Sreeedhar, J. M. Honig, M. Darwin, M. McElfresh, P. M. Shand, J. Xu, B. C. Crooker, and J. Spalek, Phys. Rev. B **46**, 6382 (1992).

[15]X. Granados *et al.* (unpublished).

[16]W. F. Brinkman and T. M. Rice, Phys. Rev. B **2**, 4302 (1970).

[17]It has been recently suggested that Eq. (6) may also hold out of the perturbative regime. X. Y. Zhang, M. J. Rozenberg, and G. Kotliar, Phys. Rev. Lett. **70**, 1666 (1993).